



Published in final edited form as:

*Angiogenesis*. 2015 October ; 18(4): 449–462. doi:10.1007/s10456-015-9468-3.

## Hypoxia-induced expression of phosducin-like 3 regulates expression of VEGFR-2 and promotes angiogenesis

Srimathi Srinivasan<sup>1</sup>, Vipul Chitalia<sup>2</sup>, Rosana D. Meyer<sup>1</sup>, Edward Hartsough<sup>1</sup>, Manisha Mehta<sup>1</sup>, Itrat Harrold<sup>3</sup>, Nicole Anderson<sup>3</sup>, Hui Feng<sup>3</sup>, Lois E. H. Smith<sup>4</sup>, Yan Jiang<sup>5</sup>, Catherine E. Costello<sup>5</sup>, and Nader Rahimi<sup>1,6</sup>

Nader Rahimi: nrahimi@bu.edu

<sup>1</sup>Departments of Pathology and Ophthalmology, Boston University School of Medicine, Boston, MA 02118, USA

<sup>2</sup>Renal Section, Department of Medicine, Boston Medical Center, Boston University School of Medicine, Boston, MA, USA

<sup>3</sup>Section of Hematology and Medical Oncology, Department of Pharmacology and Experimental Therapeutics, The Center for Cancer Research, Boston University School of Medicine, Boston, MA, USA

<sup>4</sup>Department of Ophthalmology, Boston Children's Hospital, Harvard Medical School, Boston, MA, USA

<sup>5</sup>Department of Biochemistry and Center for Biomedical Mass Spectrometry, School of Medicine, Boston University Medical Campus, Boston, MA, USA

<sup>6</sup>Department of Pathology, Boston University Medical Campus, 670 Albany St., Room 510, Boston, MA 02118, USA

### Abstract

Expression and activation of vascular endothelial growth factor receptor 2 (VEGFR-2) by VEGF ligands are the main events in the stimulation of pathological angiogenesis. VEGFR-2 expression is generally low in the healthy adult blood vessels, but its expression is markedly increased in the pathological angiogenesis. In this report, we demonstrate that phosducin-like 3 (PDCL3), a recently identified chaperone protein involved in the regulation of VEGFR-2 expression, is required for angiogenesis in zebrafish and mouse. PDCL3 undergoes N-terminal methionine acetylation, and this modification affects PDCL3 expression and its interaction with VEGFR-2. Expression of PDCL3 is regulated by hypoxia, the known stimulator of angiogenesis. The mutant PDCL3 that is unable to undergo N-terminal methionine acetylation was refractory to the effect of hypoxia. The siRNA-mediated silencing of PDCL3 decreased VEGFR-2 expression resulting in a decrease in VEGF-induced VEGFR-2 phosphorylation, whereas PDCL3 over-expression increased VEGFR-2 protein. Furthermore, we show that PDCL3 protects VEGFR-2 from misfolding and aggregation. The data provide new insights for the chaperone function of PDCL3

---

Correspondence to: Nader Rahimi, nrahimi@bu.edu.

**Conflict of interest:** The authors declare no conflict of interest.

in angiogenesis and the roles of hypoxia and N-terminal methionine acetylation in PDCL3 expression and its effect on VEGFR-2.

### Keywords

Angiogenesis; VEGFR-2; PDCL3; Hypoxia; Protein ubiquitination; N-terminal methionine acetylation; Chaperone protein

---

### Introduction

Angiogenesis, the formation of new blood vessels, plays a central role in embryonic development, wound healing, tumor growth, and neovascular ocular diseases. Proteins that promote angiogenesis play central roles in the onset and the progression of tumor progression and ocular neovascularization and retinopathies [1, 2]. The expression of a unique set of proteins in endothelial cells with pro- and anti-angiogenesis functions regulates angiogenesis, and disruption in the activity or expression of these proteins so-called angiogenic switch is responsible for pathological angiogenesis [2–4]. To maintain normal angiogenesis, endothelial cells must possess mechanisms to control the proteostasis of pro- and anti-angiogenesis proteins.

In general, the balance between endogenous pro-angiogenic and anti-angiogenic factors regulates angiogenesis, such that endothelial cell growth is normally controlled. However, in pathologic angiogenesis, a shift occurs in the balance of regulators where the expression and/or activation of pro-angiogenic factors such as VEGF and its canonical receptors is significantly upregulated, which leads to pathological angiogenesis [5–7]. VEGFR-2 is an essential mediator of VEGF-initiated angiogenesis and plays a pivotal role in regulating multiple signaling pathways in endothelial cells that modulate the core angiogenic responses including proliferation, migration, and capillary tube formation [8, 9]. VEGF-induced posttranslational modifications (PTMs) of VEGFR-2 such as tyrosine and serine/threonine phosphorylation, ubiquitination, and methylation confer VEGFR-2 as a multi-potent regulator of angiogenesis. These PTMs subsequently arbitrate the outcome of angiogenic signaling and homeostasis of the mature VEGFR-2 protein in endothelial cells [3, 10]. The abundance of mature cell surface VEGFR-2 protein is regulated primarily by the mechanisms that involve increase in both stabilization and destabilization of VEGFR-2. For example, VEGF-induced association of VEGFR-2 with protein  $\beta$ Trcp ubiquitin E3 ligase destabilizes VEGFR-2 [11], whereas its association with Ephrin-B2 and vascular endothelial cadherin inhibits its internalization and prolongs its presence at the cell surface [12, 13].

VEGFR-2 is only detectable at low levels in the adult blood vessels [14]. However, VEGFR-2 expression is markedly upregulated in blood vessels in the pathological conditions, like cancer, chronic inflammation, and wound repair [5, 6, 15]. Despite extensive research and significant clinical interest in the VEGFR-2 signaling, the molecular mechanisms governing the upregulation of VEGFR-2 in the pathological situations is not fully understood. In general, newly synthesized cell surface receptors are transported through the endoplasmic reticulum (ER) membrane in an unfolded form where molecular chaperones and other enzymes facilitate their folding and assembly into their native

conformation [16, 17]. Proteins that cannot acquire proper native folding are often kept in the ER and rapidly degraded [18, 19]. A recent study suggests that phosducin-like 3 (PDCL3) associates with VEGFR-2 and inhibits its 26S-proteasomal-dependent degradation [20]. Association of PDCL3 with VEGFR-2 increases VEGFR-2 expression and its tyrosine phosphorylation in response to VEGF stimulation [20]. PDCL3 belongs to the phosducin family of proteins, and members of the phosducin-like family proteins were initially identified as heterotrimeric G protein binding partners [21–23]. However, the biological importance of PDCL3 in the VEGFR-2 signaling and angiogenesis in particular remains unknown. In this study, we provide new insights for the previously unrecognized function of PDCL3 in angiogenesis and the role of N-terminal methionine acetylation on its function.

## Materials and methods

### Reagents and antibodies

Rabbit polyclonal anti-VEGFR-2 antibody was raised against amino acids corresponding to the kinase insert of VEGFR-2 [24]. The following antibodies were purchased from Santa Cruz Biotechnology Inc: pre-adsorbed goat anti-rabbit IgG (sc-2054), goat anti-mouse IgG (sc-2055) secondary antibodies conjugated to horseradish peroxidase, and anti-c-myc (9E10) (sc-40). Anti-PDCL3 antibody from Abcam was used for western blot analysis, and anti-PDCL3 antibody (HPA027094) from Sigma used for immunohistochemistry. ER-specific dye was purchased from Millipore. Brefeldin A (BFA) (87022601) was purchased from Sigma.

### Cell lines

HEK-293 (human embryonic kidney epithelial cells) and porcine aortic endothelial (PAE) cells were grown in DMEM medium supplemented with 10 % FBS plus antibiotics. Human umbilical vascular endothelial cells (HUVECs) were grown in the endothelial cell medium. Retroviruses were produced in 293-GPG packaging cells as described [24]. For hypoxic experiments, cells were incubated at 1 % oxygen, 95 % nitrogen, and 5 % carbon dioxide for 24 h at 37 °C.

### Cell surface biotinylation assay

HEK-293 cells expressing VEGFR-2 alone or VEGFR-2 with PDCL3 were subjected to biotinylation assay using a cell surface protein isolation kit (Cat # 89881, Pierce Biotechnology), and biotinylated proteins were purified as recommended by the manufacturer. Briefly, cells were incubated with sulfo-NHS-SS-biotin [sulfosuccinimidyl-2-(biotinamido)ethyl-1,3-dithiopropionate] for 30 min on ice. Quenching solution was added to stop biotinylation reaction, cells were lysed, and biotinylated proteins were purified by NeutrAvidin Agarose beads. The eluted biotinylated proteins were subjected to immunoprecipitation using anti-VEGFR-2 antibody.

### Mass spectrometry analysis

PDCL3 was immunoprecipitated with anti-Myc antibody from HEK-293 cells ectopically expressing PDCL3. The immunoprecipitated proteins were subjected to proteolytic digestion (incubated at 37 °C for 4 h in the presence of trypsin) on a ProGest (Genomic Solutions).

Samples were analyzed by nano-LC/MS/MS on a Thermo Fisher LTQ Orbitrap XL. Thirty microliters of hydrolysate was loaded onto a 5-mm 75- $\mu$ m ID C12 (Jupiter Proteo, Phenomenex) vented column at a flow rate of 10  $\mu$ l/min. The mass spectrometer was operated in data-dependent mode; the six most abundant ions were selected for MS/MS. The Orbitrap MS scan was performed at 60,000 FWHM resolution. MS/MS data were searched using a local copy of Mascot ([www.matrixscience.com](http://www.matrixscience.com)). Samples were processed in the Scaffold algorithm ([www.proteomesoftware.com](http://www.proteomesoftware.com)) using DAT files generated by Mascot. Parameters for LTQ Orbitrap XL data require a minimum of 2 peptides matching per protein with minimum probabilities of 90 % at the protein level and 50 % at the corresponding peptide level.

### Plasmids and siRNA

Human phosphatidylinositol-3-OH kinase class III (PI3K)  $\gamma$  cDNA (PDCL3 also called PHLPP2A) (Clone # 3344703, accession # BC001021) was purchased from Open Biosystems and was cloned into expression vectors, pcDNA3.1/Myc-His(-), or into retroviral vector, pMSCV. Mutant PDCL3 was generated by removing the first methionine and adding HA-tag and similarly was cloned into pcDNA3.1 and pMSCV vectors. Human PDCL3 siRNA (sc-94814) and mouse PDCL3 shRNA (sc-152127-SH) were purchased from Santa Cruz, Inc. The PDCL3 morpholino for zebrafish was 5'CGGTGT CTGCGTTTGGGTCCTGCAT3' and synthesized by Gene Tools, LLC. Dr. Kermit L. Carraway (UC Davis Cancer Center, Sacramento, California) generously provided the GFP-KDEL plasmid [25].

### Immunoprecipitation and western blotting

Cells were prepared and lysed as described [11]. Briefly, cells were washed twice with H/S buffer (25 mM HEPES, pH 7.4, 150 mM NaCl, and 2 mM Na<sub>3</sub>VO<sub>4</sub>) and lysed in lysis buffer (10 mM Tris-HCl, 10 % glycerol, pH 7.4, 5 mM EDTA, 50 mM NaCl, 50 mM NaF, 1 % Triton X-100, 1 mM phenylmethylsulfonyl fluoride [PMSF], 2 mM Na<sub>3</sub>VO<sub>4</sub>, and 20  $\mu$ g/ml aprotinin). Whole cell lysates were subjected to immunoprecipitation or were directly subjected to western blotting analysis as indicated in the figure legends.

### Cycloheximide-chase assay

PAE cells expressing VEGFR-2 alone or together with PDCL3 were serum-starved for overnight followed by incubation of cells with serum-free DMEM medium containing cycloheximide (20  $\mu$ g/ml, 90 min). Cells then were stimulated with VEGF for various times to downregulate cell surface VEGFR-2. Cells were lysed, and whole cell lysates blotted for VEGFR-2 using anti-VEGFR-2 antibody. Half-life of PDCL3 and HA-tagged mutant PDCL3 was measured by incubating the cells with cycloheximide (20  $\mu$ g/ml) for indicated times as shown in the figure; cells were lysed, and whole cell lysates was blotted for PDCL3.

### Protein aggregation assay

Aggregation of VEGFR-2 determined using PSA kit purchased from ProFoldin, Inc (Hudson, MA), and assay was performed according to manufacturer's guideline. PSA (8-anilino-1-naphthalenesulfonate) acts as a molecular rotor dye that rotates like a propeller

without the presence of protein aggregates and does not fluoresce. When the PSA dye binds to the aggregate, it is immobilized and slows down the rotational movement, inducing the dye to fluoresce. In brief, VEGFR-2 immunoprecipitated from HEK-293 cells and eluted from the protein-Sepharose beads. The eluted VEGFR-2 protein was incubated at 45 °C in the presence or absence of purified GST-PDCL3 for various time points. The fluorescence intensity was measured at 610 nm.

### **Immunofluorescence microscopy**

HEK-293 cells expressing Myc-tagged PDCL3 or co-expressed with GFP-KDEL were grown in chamber slides. The slides were fixed in ice-cold methanol for 10 min at room temperature after washing once with TBS buffer. The slides were blocked with 1 % BSA in TBS buffer for 30 min followed by incubation with the primary antibody against human PDCL3 and ER-specific dye in 1 % BSA in TBS for 2 h. The mixture solution was decanted, and the slides were washed with TBS. The slides then were incubated with the mouse FITC-conjugated secondary antibody in 1 % BSA with TBS for 1 h. The secondary antibody solution was then decanted and washed three times with TBS for 5 min each. The slides were mounted with mounting media with DAPI. The images were taken using Nikon deconvolution wide-field Epifluorescence system.

### **Hypoxia-induced mouse angiogenesis**

All experiments were performed in accordance with the NIH Guide for the Care and Use of Laboratory Animals. All the experimental procedures were approved by the Children Hospital Animal Care and Use Committee. Oxygen-induced retinopathy (OIR) of prematurity was induced in C57BL/6J mice according to the protocol described [26]. Briefly, postnatal day 7 (P7) pups and their mothers were transferred from normal air to an environment of 75 % oxygen for 5 days and afterward returned to room air. Abnormal pre-retinal neovascularization occurs after return to normoxia starting at around P17. The eye tissue used in this study was P17.

### **Mouse matrigel-plug angiogenesis assay**

Matrigel-plug angiogenesis was performed as described [27]. Mice (six animals for each experimental group) were injected with matrigel (10 mg/ml), VEGF (100 ng) plus a control retrovirus shRNA or PDCL3 shRNA. Retroviruses were prepared as described [24]. The animals were sedated with Avertin (0.3 ml per 20-g mouse), and a 25-gauge needle was used to inject matrigel mixture (200 µl) subdermally into mice. After 8 days, animals were killed, matrigel plugs were removed, and plugs were homogenized in 1 ml of deionized water on ice and cleared by centrifugation at 10,000 rpm for 5 min at 4 °C. The supernatant was collected and used to measure hemoglobin content with Drabkin's reagent along with hemoglobin standards as suggested by the manufacturer (Sigma-Aldrich, St. Louis, MO), and the absorbance was read at 540 nm [28].

### **Synthesis of capped mRNA**

The PDCL3 and VEGFR-2 plasmids were linearized with Not I restriction enzyme. Linearized plasmids (1 µg/µl) were used for in vitro capped mRNA synthesis using the

mMessage mMachine<sup>®</sup> SP6 kit (Ambion) according to manufacturer instructions, and RNA subsequently were used to inject into zebrafish embryos.

### Zebrafish angiogenesis assay

Fli-eGFP-transgenic adult male and female zebrafish (*Danio rerio*) were housed in 14:19-h light–dark cycle at a temperature of (26.5 °C) and a pH of (7.0–7.4) in a controlled multi-tank recirculating water system (Aquatic Habitats, Apopka, FL). A glass capillary needle attached to a Femtojet injector (Eppendorf) was used for injecting RNA (10 or 5 ng/μl in approximately 10 pl) into one- or two-cell-stage embryos. The embryos were grown at 28 °C for 3 days. The embryos were examined after 28 or 50 h post-injection (hpf) using Zeiss immunofluorescence microscope. The images of fish under the same light exposure setting were obtained for ten randomly selected fish per group at every experiment and analyzed for the length of the tail vessels. The vessels were marked from the junction of the body and the tail going caudally using Image-Pro<sup>®</sup> and averaged per group, as described previously [10].

### RT-PCR

Zebrafish embryos are harvested at 28 h post-fertilization and subjected to total RNA extraction using RNashredder and RNeasy (Qiagen, Inc). RT-qPCR (reverse transcription quantitative PCR) was performed as recommended by the manufacturer (Applied Biosystems) and 18S used as internal controls.

### Statistical analysis

Western blots and in vitro angiogenesis assays were quantified using Image J software. Zebrafish blood vessel quantification was performed as described [10]. In short, ten fish per group at every experiment were analyzed for the length of the caudal vein plexus formation using Image-Pro<sup>®</sup> software. Wilcoxon rank-sum test was used to compare blood vessel formation in zebrafish. Immunohistochemistry staining of PDCL3 was quantified by Image J software.

## Results

### PDCL3 is located at the ER and promotes VEGFR-2 expression by protecting it from misfolding

PDCL3 was recently identified as a chaperone protein that associates with VEGFR-2 and inhibits its ubiquitination and degradation [20]. However, the molecular mechanisms such as cellular location where PDCL3 recognizes and interacts with VEGFR-2 remain unknown. We used a cell surface biotinylation assay to determine whether PDCL3 interacts with the cell surface or with the intracellular pool of VEGFR-2. The result showed that PDCL3 interacts primarily with the intracellular VEGFR-2 (Fig. 1a). To determine whether PDCL3 binds to VEGFR-2 at the ER compartments, we inhibited the anterograde transport of proteins from the ER to the Golgi apparatus with brefeldin A (BFA) [29, 30] and assessed the binding of PDCL3 with VEGFR-2. Treatment of cells with BFA did not inhibit the binding of PDCL3 with VEGFR-2 (Fig. 1b), suggesting that PDCL3 recognizes VEGFR-2 during synthesis or just after its initial synthesis at the ER compartments.

To initially examine the cellular localization of PDCL3, we used immunofluorescence microscopy and show that PDCL3 is present in the perinuclear/cytoplasmic areas of cells (Fig. 1c). The staining of cells with an ER-specific tracking dye showed that PDCL3 is localized at both the ER and the cytoplasmic compartments (Fig. 1d). Additionally, PDCL3 was co-localized with GFP-tagged KDEL, an ER/Golgi marker (Fig. 1e). Consistent with the immunofluorescence microscopy data, cellular fractionation of cells expressing PDCL3 also showed the presence of PDCL3 in the ER compartments (data not shown). Taken together, the data demonstrate that PDCL3 is present at both ER and non-ER compartments.

Chaperone proteins interact with the newly synthesized nascent proteins and assist the folding/maturation [31]. To investigate the effect of PDCL3 on VEGFR-2, we initially co-expressed PDCL3 with VEGFR-2 with varying concentrations of PDCL3 and evaluated the effect of overexpression of PDCL3 on the VEGFR-2 protein levels. The data showed that increasing the expression of PDCL3 in HEK-293 cells promotes upregulation of VEGFR-2 (Fig. 2a). To examine the functional importance of endogenous PDCL3 on the expression of VEGFR-2 in primary endothelial cells, we silenced the expression of PDCL3 by siRNA and assessed the expression of VEGFR-2 and its tyrosine phosphorylation in response to VEGF stimulation. Silencing PDCL3 significantly reduced the expression of VEGFR-2, and as a result, its tyrosine phosphorylation in response to VEGF stimulation was significantly diminished (Fig. 2b). To investigate further the chaperone function of PDCL3 on VEGFR-2, we next examined whether PDCL3 could increase the yield of VEGFR-2 protein production in a cell-free in vitro translation system. Addition of recombinant PDCL3 protein into an in vitro translation mixture significantly increased (12-fold) the yield of in vitro-translated VEGFR-2 (Fig. 2c), further supporting the chaperone function of PDCL3 on VEGFR-2.

Molecular chaperones are thought to regulate protein stability by preventing aggregation of partially unfolded proteins and maintaining partially unfolded proteins in a state of competent for refolding [32]. To determine whether PDCL3 plays a role in the folding of VEGFR-2, we measured the heat-induced aggregation of VEGFR-2 in the presence of recombinant PDCL3. Incubation of immunoprecipitated VEGFR-2 with PDCL3 at 45 °C significantly reduced aggregation of VEGFR-2 in a time-dependent manner (Fig. 2d), indicating that PDCL3 assists the folding of VEGFR-2.

We next tested the effect of PDCL3 on stability of VEGFR-2 in vitro cell culture system. To this end, we treated cells expressing VEGFR-2 alone or co-expressing with PDCL3 with protein synthesis inhibitor, cycloheximide, followed by stimulation of cells with VEGF for various time points. Cells were stimulated with VEGF to downregulate the mature cell surface VEGFR-2. Ligand stimulation rapidly downregulates VEGFR-2 and reduces its cell surface expression [11, 33]. Cycloheximide treatment inhibited VEGFR-2 protein synthesis as the presence of newly synthesized VEGFR-2 (low molecular weight) was diminished as function of time (Fig. 3b). The same treatment had a minor effect on the newly synthesized VEGFR-2 in the cells co-expressing VEGFR-2 with PDCL3 (Fig. 3b). The presence of newly synthesized VEGFR-2 persisted even when cells were treated with VEGF (Fig. 2b). The presence of mature VEGFR-2 and the rate of its downregulation in response to VEGF were similar in the cells expressing VEGFR-2 alone or co-expressing with PDCL3 when cells were treated with CHX (Fig. 3B). However, in the absence of CHX treatment, the

levels of the mature VEGFR-2 were considerably decreased during the time course of VEGF stimulation, whereas levels of the mature VEGFR-2 were substantially remained higher in the cells over-expressing PDCL3 (Fig. 3b). The levels of the mature VEGFR-2 at the 60 min stimulation with VEGF were similar in both the groups, indicating that the mature VEGFR-2 was downregulated in response to VEGF stimulation (Fig. 3b). In addition, levels of newly synthesized VEGFR-2 were higher in the cells over-expressing PDCL3 and VEGF stimulation had only a minor effect on its levels (Fig. 3c). Altogether, the data demonstrate that PDCL3 increases VEGFR-2 expression by stabilization and maturation of newly synthesized VEGFR-2.

### PDCL3 promotes angiogenesis in mouse and zebrafish

We next used mouse matrigel-plug angiogenesis assay to investigate the biological importance of PDCL3 in VEGF-induced angiogenesis. The data showed that the VEGF containing matrigel-plug plus control shRNA stimulated angiogenesis. However, the VEGF containing matrigel-plug plus *PDCL3* shRNA significantly inhibited the VEGF-induced angiogenesis (Fig. 4a, b). The effect of *PDCL3* shRNA on the expression of PDCL3 and VEGFR-2 also is shown (Fig. 4c). To investigate the in vivo importance of PDCL3 in angiogenesis further, we decided to examine angiogenesis in zebrafish. We used zebrafish to study angiogenesis due to its high conservation to humans and genetic and imaging capabilities [34, 35]. Microinjection of in vitro-translated human *PDCL3* mRNA into one-stage zebrafish embryos significantly increased blood vessel formation in a dose-dependent manner as formation of tail vessel length was increased (Fig. 5a). Quantification of the tail blood vessel formation in response to microinjection of human *pdcl3* mRNA is shown (Fig. 5b). Western blot analysis was performed to confirm the over-expression of PDCL3 in microinjected fishes (Fig. 5c).

To determine the functional importance of the endogenous PDCL3 in angiogenesis, we silenced the expression of zebrafish *pdcl3* by morpholino and examined the blood vessel formation in zebrafish. Silencing *pdcl3* in zebrafish by morpholino significantly inhibited angiogenesis as noted by the reduction in tail vessel formation (Fig. 5d, e). Co-injection of *pdcl3* morpholino with *VEGFR-2* mRNA markedly rescued the effect of *pdcl3* knockdown (Fig. 5d, e), indicating that VEGFR-2 is the primary downstream target of PDCL3 in endothelial cells. Although over-expression and silencing of *pdcl3* expression in zebrafish underscore the biological importance of PDCL3 in angiogenesis, given the nature of these injections, the effects of PDCL3 on the other cell types during the embryonic development of fish cannot be excluded. The effect of *pdcl3* morpholino on the expression of zebrafish PDCL3 was confirmed by qPCR (Fig. 5f). Western blot analysis also confirmed over-expression of VEGFR-2 in the microinjected fishes with VEGFR-2 mRNA (Fig. 5f). Taken together, the data demonstrate that PDCL3 activity is required for angiogenesis in mouse and zebrafish.

### Hypoxia increases expression of PDCL3

Because PDCL3 regulates the abundance of VEGFR-2 and angiogenesis in mouse and zebrafish, we decided to examine whether the expression of PDCL3 in conditions that mimics pathological angiogenesis such as hypoxia is the best-known trigger of pathological



angiogenesis [36, 37]. VEGFR-2 is generally expressed at low levels in most adult vessels, but its expression is strongly upregulated in the pathological circumstances such as hypoxia and ischemic conditions [38, 39]. To examine the effect of hypoxia on the expression of PDCL3 *in vivo*, we initially examined the expression of PDCL3 in a well-characterized mouse model of hypoxia-induced angiogenesis [40]. In this model, the maximum ocular neovascularization is observed at the postnatal day 17, P17 [26]. Immunohistochemistry analysis of ocular tissues showed that the expression of PDCL3 is highly upregulated in response to hypoxia, particularly in the blood vessels of the retina (Fig. 6a). Expression of PDCL3 was relatively undetectable in normal mouse retinal tissue (Fig. 6a). Similarly, the expression of VEGFR-2 also was significantly higher in the mouse ocular tissue exposed to hypoxia (Fig. 6a). The data demonstrate that hypoxia promotes expression of both PDCL3 and VEGFR-2.

To demonstrate the effect of hypoxia on the PDCL3 expression, we exposed endothelial cells to hypoxic environment (1 % oxygen, 24 h) and evaluated the expression of PDCL3 and VEGFR-2. Hypoxia significantly increased the expression of PDCL3 (Fig. 6b). Similarly, the expression of VEGFR-2 also was markedly increased in response to hypoxia (Fig. 6b). Moreover, ubiquitination of VEGFR-2 in cells exposed to hypoxia was substantially reduced (Fig. 6b), indicating that the reduction in the ubiquitination of VEGFR-2 may contribute to elevated expression of VEGFR-2. Treatment of cells with cobalt chloride, which mimics the effect of hypoxia, similarly increased the expression of PDCL3 and VEGFR-2 (data not shown). To determine whether the increased expression of VEGFR-2 in response to hypoxia is associated with the upregulation of PDCL3, we silenced PDCL3 by siRNA and measured the VEGFR-2 levels. The knockdown of PDCL3 inhibited the hypoxia-mediated upregulation of VEGFR-2 (Fig. 6c). Altogether, the data show that hypoxia promotes PDCL3 expression and that elevated expression of PDCL3 in part mediates the hypoxia-mediated upregulation of VEGFR-2.

### **N-terminal methionine acetylation regulates PDCL3 degradation**

To determine the mechanism by which hypoxia promotes upregulation of PDCL3, we analyzed possible PTMs on PDCL3 by liquid chromatography–tandem mass spectrometry (LC–MS/MS) analysis. Our analysis revealed that PDCL3 was acetylated on the N-terminal methionine (Fig. 7a). Recently, the N-terminal methionine acetylation was recognized as a novel mechanism to regulate protein stability by serving as a degradation signal so-called N-degron [41]. To examine the role of N-terminal methionine acetylation in PDCL3 stability, we generated an acetylation-resistant PDCL3 construct by inserting an HA-tag at the N-terminal of PDCL3 (Fig. 7b). Despite using an equal amount of DNA constructs, the expression of HA-tagged PDCL3 was higher compared to the expression of wild-type PDCL3 (Fig. 7b).

Provided that the N-terminal acetylation has a destabilizing effect on the target proteins [42], we carried out a cycloheximide (CHX)-chase assay and analyzed the half-life of PDCL3. Half-life of the wild-type PDCL3 was relatively short (about 30 min), whereas the acetylation-resistant HA-tagged PDCL3 was quite stable and its half-life was about 60 min

(Fig. 7c), indicating that the N-terminal methionine acetylation destabilizes PDCL3 and preventing its acetylation increases its half-life.

Given that hypoxia promotes the expression of PDCL3, we analyzed possible role of the N-terminal methionine acetylation in PDCL3 expression in response to hypoxia. Cells expressing wild-type PDCL3 or acetylation-resistant HA-tagged PDCL3 were incubated in hypoxic environment for 24 h, and the expression of PDCL3 was determined in western blot analysis. The result showed that the acetylation-resistant HA-tagged PDCL3 was refractory to the effect hypoxia (Fig. 7d), further supporting the destabilizing effect of N-terminal acetylation on PDCL3. To test whether acetylation-resistant HA-tagged PDCL3 also interacts with and reduces ubiquitination of VEGFR-2, we determined its binding with VEGFR-2 and ubiquitination of VEGFR-2. The acetylation-resistant HA-tagged PDCL3 interacted strongly with VEGFR-2 compared to the wild-type PDCL3 (Fig. 7e). Ubiquitination of VEGFR-2 was substantially less (Fig. 7e), indicating that the acetylation-resistant PDCL3 is more protective of VEGFR-2 than the wild-type PDCL3.

Because the acetylation-resistant HA-tagged PDCL3 strongly binds to VEGFR-2 and effectively reduces VEGFR-2 ubiquitination, we decided to examine whether over-expression of acetylation-resistant HA-tagged PDCL3 in endothelial cells could increase the VEGFR-2-dependent tube formation. Over-expression of the both wild-type and acetylation-resistant HA-tagged PDCL3 in endothelial cells increased angiogenesis/capillary tube formation, but the effect of acetylation-resistant HA-tagged PDCL3 on the tube formation was more robust (Fig. 7f). Taken together, the data demonstrate that PDCL3 undergoes N-terminal methionine acetylation, and this PTM plays an important role in its expression and function in endothelial cells.

## Discussion

Angiogenesis, the development of new blood vessels from preexisting vasculature, contributes to the onset and the development of various human diseases ranging from cancer to neovascular eye disorders [1, 2]. A remarkable feature of angiogenesis is the ability of endothelial cells to proliferate rapidly in the pathological circumstances, such as tumorigenesis, by increasing the expression of various angiogenic factors and others [38]. Intratumoral hypoxia promotes over-expression of the VEGF ligands in tumor cells and its tyrosine kinase receptors, particularly, VEGFR-2 in tumors and tumor-associated endothelium [43–45]. Upregulation of VEGFR-2 in various preclinical and clinical studies has been documented [45–48], and whether the expression of VEGFR-2 also is regulated by posttranslational events is less understood.

The work described here has uncovered PDCL3, a protein with a chaperone activity, as a key regulator of VEGFR-2 protein stability. These findings constitute a significant advance in our understanding of how hypoxia stimulates the expression of VEGFR-2 by posttranslational mechanism. Interfering with the expression of PDCL3 both in zebrafish and mouse angiogenesis models inhibited angiogenesis, indicating that PDCL3 activity plays a vital role in angiogenesis in vivo. PDCL3 appears to regulate angiogenesis by modulating the expression of VEGFR-2. Over-expression of VEGFR-2 in zebrafish was

able to rescue the effect of *pdcl3* morpholino, indicating that VEGFR-2 is the primary target of PDCL3 in endothelial cells. However, PDCL3 could play a broader role in angiogenesis by affecting the expression of other angiogenic factors.

Previously, PDCL3 was described as a cytoplasmic protein, and our observation demonstrates that PDCL3 is present at both the ER and cytoplasmic compartments. Various probes, including ER-tracking dye and ER-specific marker, KDEL and brefeldin A, a chemical that inhibits the anterograde transport of proteins from the ER to the Golgi apparatus, all demonstrate that in addition to cytoplasmic compartments, PDCL3 also is present at the ER. Chaperone proteins such as Hsp90s are present in various cellular compartments including ER, mitochondria, and cytoplasm [49]. The ER localized Hsp90 chaperone proteins associate with and assist with the appropriate folding of nascent proteins [50]. Consistent with the chaperone function of PDCL3, the ER localized PDCL3 associates with the newly synthesized VEGFR-2 and protects from degradation. Consistent with this observation, our study has shown that over-expression of PDCL3 increases, whereas silencing its expression by siRNA significantly decreases the expression of VEGFR-2. Similarly, depletion of PDCL3 increased ubiquitination of VEGFR-2, and its over-expression reduced the ubiquitylation of VEGFR-2 [20].

Although recently N-terminal acetylation has been suggested to play a role in protein stability through the N-end rule pathway [41], to date, the role of N-terminal acetylation in mammalian cells remains poorly understood. Our data demonstrate that N-terminal methionine acetylation regulates the stability of PDCL3 and as a result VEGFR-2 expression, a key receptor tyrosine kinase whose activity is associated with pathological angiogenesis such as cancer and various other diseases. PDCL3 stability appears to play an important role in angiogenesis, as its expression was upregulated by hypoxia, a master regulator of angiogenesis [20]. Furthermore, zebrafish and mouse experiments confirmed the biological importance of PDCL3 in angiogenesis. Over-expression of PDCL3 in zebrafish increased, and depleting its expression by morpholino inhibited angiogenesis. Similarly, over-expression of mutant PDCL3 that is unable to undergo N-terminal acetylation showed more potent activity than the wild-type PDCL3 to stimulate angiogenesis, underscoring the biological significance of N-terminal acetylation in its function.

N-terminal acetylation is considered a co-translational event and is likely irreversible [42]. At this time, it remains unclear how hypoxia modulates the N-terminal acetylation of PDCL3. A mutant form of PDCL3 unable to undergo N-terminal acetylation is refractory to the effect of hypoxia, indicating that hypoxia, in part, might promote stability of PDCL3 by inhibiting the acetylation of PDCL3. Given that N-terminal acetylation is considered a non-reversible PTM [41], and consistent with this notion, our quantitative MS analysis also showed that acetylation of PDCL3 is not inhibited by hypoxia (data not shown). One possible mechanism by which hypoxia could modulate the stability of PDCL3 is through inhibition of expression or activity of ubiquitin E3 ligase enzymes involved in the recognition of N-degron motif of PDCL3 that might target PDCL3 to ubiquitination-dependent proteasomal degradation.

In summary, the work presented in this manuscript suggests that perturbation in the proteostasis of VEGFR-2 involving PDCL3 could lead to increased angiogenesis. The observation that PDCL3 expression is regulated by hypoxia and plays an important role in stability of VEGFR-2 and angiogenesis appears to be part of the hypoxia-sensing mechanism evolved to maintain physiological angiogenesis, and dysregulation of this mechanism could lead to an unwanted angiogenesis. Given that the current anti-angiogenesis therapies due to insufficient efficacy, intrinsic refractoriness, and development of resistance have only limited therapeutic benefits in cancer treatment, the data presented in this manuscript suggest that interfering with the PDCL3 activity, in principal, could increase the efficacy of anti-angiogenesis drugs. Future studies will address whether the altered endothelial-specific expression of PDCL3 could lead to aberrant angiogenesis and disease.

## Acknowledgments

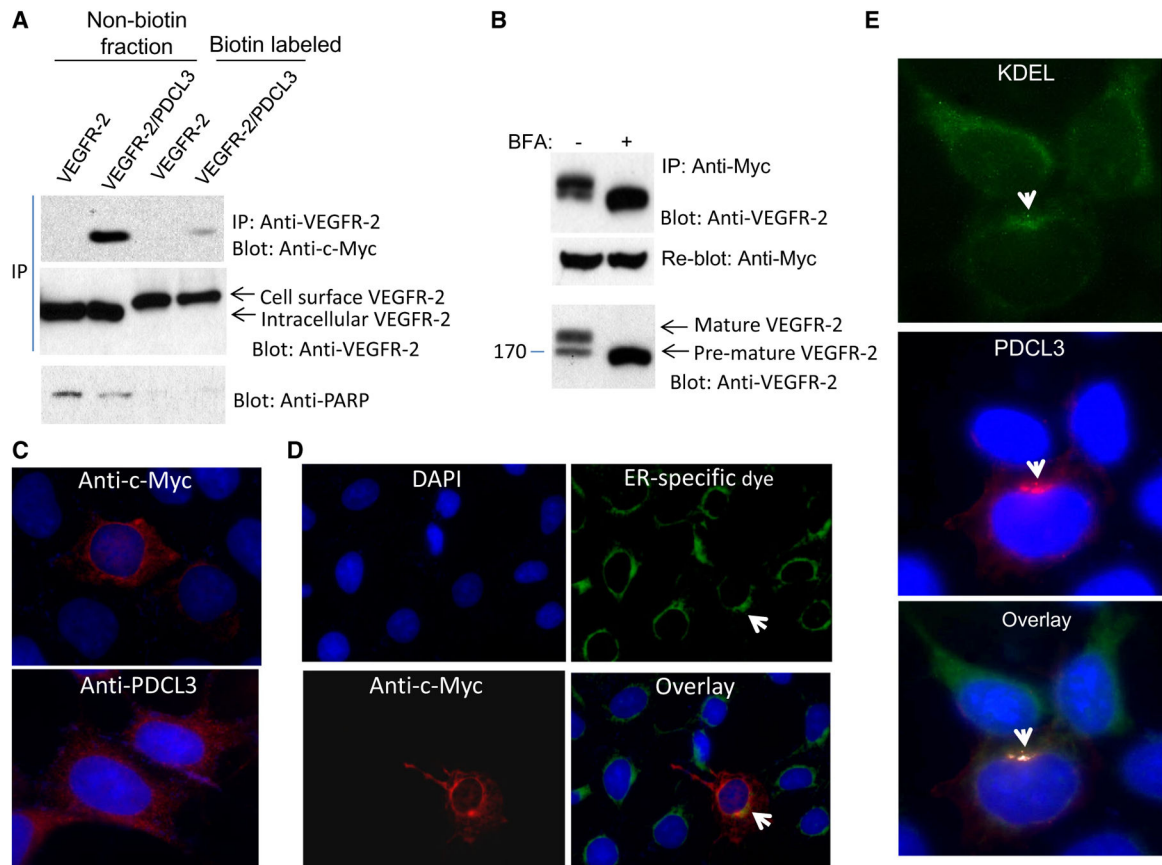
This work was supported in part through a grant from the NIH/National Eye Institute (R01EY017955 to N. R.); P41 RR010888/GM104603, S10 RR020946, and NIH/National Heart, Lung, and Blood Institute contract N01 HHSN268201000031C (to C. E. C.); and K08 award (NIH/National Institute of Diabetes and Digestive and Kidney Diseases DK080946 and Department of Medicine Career Investment Award to V. C.).

## References

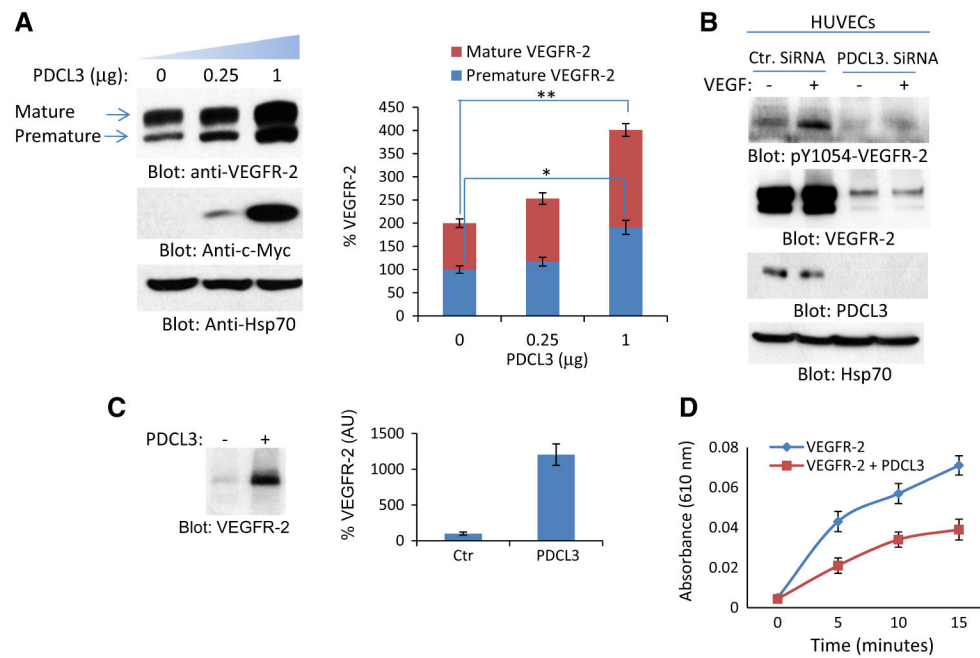
1. Carmeliet P. Angiogenesis in life, disease and medicine. *Nature*. 2005; 438(7070):932–936.10.1038/nature04478 [PubMed: 16355210]
2. Carmeliet P, Jain RK. Molecular mechanisms and clinical applications of angiogenesis. *Nature*. 2011; 473(7347):298–307.10.1038/nature10144 [PubMed: 21593862]
3. Rahimi N. The ubiquitin-proteasome system meets angiogenesis. *Mol Cancer Ther*. 2012; 11(3): 538–548.10.1158/1535-7163.MCT-11-0555 [PubMed: 22357635]
4. Folkman J. Role of angiogenesis in tumor growth and metastasis. *Semin Oncol*. 2002; 29(6 Suppl 16):15–18.10.1053/sonc.2002.37263 [PubMed: 12516034]
5. Ferrara N. Vascular endothelial growth factor: molecular and biological aspects. *Curr Top Microbiol Immunol*. 1999; 237:1–30. [PubMed: 9893343]
6. Shibuya M, Luo JC, Toyoda M, Yamaguchi S. Involvement of VEGF and its receptors in ascites tumor formation. *Cancer Chemother Pharmacol*. 1999; 43(Suppl):S72–S77. [PubMed: 10357563]
7. Carmeliet P. Angiogenesis in health and disease. *Nat Med*. 2003; 9(6):653–660.10.1038/nm0603-653 [PubMed: 12778163]
8. Rahimi N. VEGFR-1 and VEGFR-2: two non-identical twins with a unique physiognomy. *Front Biosci J Virtual Libr*. 2006; 11:818–829.
9. Matsumoto T, Claesson-Welsh L. VEGF receptor signal transduction. *Sci STKE*. 2001; 2001(112): 21.10.1126/stke.2001.112.re21
10. Hartsough EJ, Meyer RD, Chitalia V, Jiang Y, Marquez VE, Zhdanova IV, Weinberg J, Costello CE, Rahimi N. Lysine methylation promotes VEGFR-2 activation and angiogenesis. *Sci Signal*. 2013; 6(304):ra104.10.1126/scisignal.2004289 [PubMed: 24300896]
11. Meyer RD, Srinivasan S, Singh AJ, Mahoney JE, Gharahassanlou KR, Rahimi N. PEST motif serine and tyrosine phosphorylation controls vascular endothelial growth factor receptor 2 stability and downregulation. *Mol Cell Biol*. 2011; 31(10):2010–2025.10.1128/MCB.01006-10 [PubMed: 21402774]
12. Sawamiphak S, Seidel S, Essmann CL, Wilkinson GA, Pitulescu ME, Acker T, Acker-Palmer A. Ephrin-B2 regulates VEGFR2 function in developmental and tumour angiogenesis. *Nature*. 2010; 465(7297):487–491.10.1038/nature08995 [PubMed: 20445540]
13. Lampugnani MG, Orsenigo F, Gagliani MC, Tacchetti C, Dejana E. Vascular endothelial cadherin controls VEGFR-2 internalization and signaling from intracellular compartments. *J Cell Biol*. 2006; 174(4):593–604.10.1083/jcb.200602080 [PubMed: 16893970]

14. Detmar M. Molecular regulation of angiogenesis in the skin. *J Invest Dermatol.* 1996; 106(2):207–208. [PubMed: 8601716]
15. Schmidt T, Carmeliet P. Angiogenesis: a target in solid tumors, also in leukemia? *Hematology Am Soc Hematol Educ Program.* 2011; 2011:1–8.10.1182/asheducation-2011.1.1 [PubMed: 22160005]
16. Bass J, Chiu G, Argon Y, Steiner DF. Folding of insulin receptor monomers is facilitated by the molecular chaperones calnexin and calreticulin and impaired by rapid dimerization. *J Cell Biol.* 1998; 141(3):637–646. [PubMed: 9566965]
17. Young JC, Agashe VR, Siegers K, Hartl FU. Pathways of chaperone-mediated protein folding in the cytosol. *Nat Rev Mol Cell Biol.* 2004; 5(10):781–791.10.1038/nrm1492 [PubMed: 15459659]
18. Hampton RY. ER-associated degradation in protein quality control and cellular regulation. *Curr Opin Cell Biol.* 2002; 14(4):476–482. [PubMed: 12383799]
19. Kostova Z, Wolf DH. For whom the bell tolls: protein quality control of the endoplasmic reticulum and the ubiquitin-proteasome connection. *EMBO J.* 2003; 22(10):2309–2317.10.1093/emboj/cdg227 [PubMed: 12743025]
20. Srinivasan S, Meyer RD, Lugo R, Rahimi N. Identification of PDCL3 as a novel chaperone protein involved in the generation of functional VEGF receptor 2. *J Biol Chem.* 2013; 288(32):23171–23181.10.1074/jbc.M113.473173 [PubMed: 23792958]
21. Flanary PL, DiBello PR, Estrada P, Dohlman HG. Functional analysis of Plp1 and Plp2, two homologues of phosducin in yeast. *J Biol Chem.* 2000; 275(24):18462–18469.10.1074/jbc.M002163200 [PubMed: 10749875]
22. Blaauw M, Knol JC, Kortholt A, Roelofs J, Ruchira Postma M, Visser AJ, van Haastert PJ. Phosducin-like proteins in *Dictyostelium discoideum*: implications for the phosducin family of proteins. *EMBO J.* 2003; 22(19):5047–5057.10.1093/emboj/cdg508 [PubMed: 14517243]
23. Humrich J, Bermel C, Bunemann M, Harmark L, Frost R, Qwitterer U, Lohse MJ. Phosducin-like protein regulates G-protein beta gamma folding by interaction with tailless complex polypeptide-1 alpha: dephosphorylation or splicing of PhLP turns the switch toward regulation of G beta gamma folding. *J Biol Chem.* 2005; 280(20):20042–20050.10.1074/jbc.M409233200 [PubMed: 15745879]
24. Rahimi N, Dayanir V, Lashkari K. Receptor chimeras indicate that the vascular endothelial growth factor receptor-1 (VEGFR-1) modulates mitogenic activity of VEGFR-2 in endothelial cells. *J Biol Chem.* 2000; 275(22):16986–16992.10.1074/jbc.M000528200 [PubMed: 10747927]
25. Fry WH, Simion C, Sweeney C, Carraway KL 3rd. Quantity control of the ErbB3 receptor tyrosine kinase at the endoplasmic reticulum. *Mol Cell Biol.* 2011; 31(14):3009–3018.10.1128/MCB.05105-11 [PubMed: 21576364]
26. Stahl A, Connor KM, Sapieha P, Chen J, Dennison RJ, Krah NM, Seaward MR, Willett KL, Aderman CM, Guerin KI, Hua J, Lofqvist C, Hellstrom A, Smith LE. The mouse retina as an angiogenesis model. *Invest Ophthalmol Vis Sci.* 2010; 51(6):2813–2826.10.1167/iovs.10-5176 [PubMed: 20484600]
27. Akhtar N, Dickerson EB, Auerbach R. The sponge/matrigel angiogenesis assay. *Angiogenesis.* 2002; 5(1–2):75–80. [PubMed: 12549862]
28. Rahimi N, Rezazadeh K, Mahoney JE, Hartsough E, Meyer RD. Identification of IGPR-1 as a novel adhesion molecule involved in angiogenesis. *Mol Biol Cell.* 2012; 23(9):1646–1656.10.1091/mbc.E11-11-0934 [PubMed: 22419821]
29. Klausner RD, Donaldson JG, Lippincott-Schwartz J, Brefeldin A: insights into the control of membrane traffic and organelle structure. *J Cell Biol.* 1992; 116(5):1071–1080. [PubMed: 1740466]
30. Helms JB, Rothman JE. Inhibition by brefeldin A of a Golgi membrane enzyme that catalyses exchange of guanine nucleotide bound to ARF. *Nature.* 1992; 360(6402):352–354.10.1038/360352a0 [PubMed: 1448152]
31. Frydman J. Folding of newly translated proteins in vivo: the role of molecular chaperones. *Annu Rev Biochem.* 2001; 70:603–647.10.1146/annurev.biochem.70.1.603 [PubMed: 11395418]
32. Hendrick JP, Langer T, Davis TA, Hartl FU, Wiedmann M. Control of folding and membrane translocation by binding of the chaperone DnaJ to nascent polypeptides. *Proc Natl Acad Sci USA.* 1993; 90(21):10216–10220. [PubMed: 8234279]

33. Singh AJ, Meyer RD, Band H, Rahimi N. The carboxyl terminus of VEGFR-2 is required for PKC-mediated down-regulation. *Mol Biol Cell*. 2005; 16(4):2106–2118.10.1091/mbc.E04-08-0749 [PubMed: 15673613]
34. Serbedzija GN, Flynn E, Willett CE. Zebrafish angiogenesis: a new model for drug screening. *Angiogenesis*. 1999; 3(4):353–359. [PubMed: 14517415]
35. Nicoli S, Ribatti D, Cotelli F, Presta M. Mammalian tumor xenografts induce neovascularization in zebrafish embryos. *Cancer Res*. 2007; 67(7):2927–2931.10.1158/0008-5472.CAN-06-4268 [PubMed: 17409396]
36. Millauer B, Wizigmann-Voos S, Schnurch H, Martinez R, Moller NP, Risau W, Ullrich A. High affinity VEGF binding and developmental expression suggest Flk-1 as a major regulator of vasculogenesis and angiogenesis. *Cell*. 1993; 72(6):835–846. [PubMed: 7681362]
37. Heidenreich R, Rocken M, Ghoreschi K. Angiogenesis: the new potential target for the therapy of psoriasis? *Drug News Perspect*. 2008; 21(2):97–105. [PubMed: 18389101]
38. Pugh CW, Ratcliffe PJ. Regulation of angiogenesis by hypoxia: role of the HIF system. *Nat Med*. 2003; 9(6):677–684.10.1038/nm0603-677 [PubMed: 12778166]
39. Rahimi N. A role for protein ubiquitination in VEGFR-2 signalling and angiogenesis. *Biochem Soc Trans*. 2009; 37(Pt 6):1189–1192.10.1042/BST0371189 [PubMed: 19909244]
40. Smith LE. Pathogenesis of retinopathy of prematurity. *Growth Horm IGF Res Off J Growth Horm Res Soc Int IGF Res Soc*. 2004; 14(Suppl A):S140–S144.10.1016/j.ghir.2004.03.030
41. Hwang CS, Shemorry A, Varshavsky A. N-terminal acetylation of cellular proteins creates specific degradation signals. *Science*. 2010; 327(5968):973–977.10.1126/science.1183147 [PubMed: 20110468]
42. Hwang CS, Shemorry A, Auerbach D, Varshavsky A. The N-end rule pathway is mediated by a complex of the RING-type Ubr1 and HECT-type Ufd4 ubiquitin ligases. *Nat Cell Biol*. 2010; 12(12):1177–1185.10.1038/ncb2121 [PubMed: 21076411]
43. Tang N, Wang L, Esko J, Giordano FJ, Huang Y, Gerber HP, Ferrara N, Johnson RS. Loss of HIF-1alpha in endothelial cells disrupts a hypoxia-driven VEGF autocrine loop necessary for tumorigenesis. *Cancer Cell*. 2004; 6(5):485–495.10.1016/j.ccr.2004.09.026 [PubMed: 15542432]
44. Ferrara N. Vascular endothelial growth factor: basic science and clinical progress. *Endocr Rev*. 2004; 25(4):581–611.10.1210/er.2003-0027 [PubMed: 15294883]
45. Heidenreich R, Murayama T, Silver M, Essl C, Asahara T, Rocken M, Breier G. Tracking adult neovascularization during ischemia and inflammation using Vegfr2-LacZ reporter mice. *J Vasc Res*. 2008; 45(5):437–444.10.1159/000126106 [PubMed: 18418002]
46. Kremer C, Breier G, Risau W, Plate KH. Up-regulation of flk-1/vascular endothelial growth factor receptor 2 by its ligand in a cerebral slice culture system. *Cancer Res*. 1997; 57(17):3852–3859. [PubMed: 9288799]
47. dela Paz NG, Walshe TE, Leach LL, Saint-Geniez M, D'Amore PA. Role of shear-stress-induced VEGF expression in endothelial cell survival. *J Cell Sci*. 2012; 125(Pt 4):831–843.10.1242/jcs.084301 [PubMed: 22399811]
48. Schmidt T, Carmeliet P. Blood-vessel formation: bridges that guide and unite. *Nature*. 2010; 465(7299):697–699.10.1038/465697a [PubMed: 20535192]
49. Kim YE, Hipp MS, Bracher A, Hayer-Hartl M, Hartl FU. Molecular chaperone functions in protein folding and proteostasis. *Annu Rev Biochem*. 2013; 82:323–355.10.1146/annurev-biochem-060208-092442 [PubMed: 23746257]
50. Hendrick JP, Hartl FU. Molecular chaperone functions of heat-shock proteins. *Annu Rev Biochem*. 1993; 62:349–384.10.1146/annurev.bi.62.070193.002025 [PubMed: 8102520]

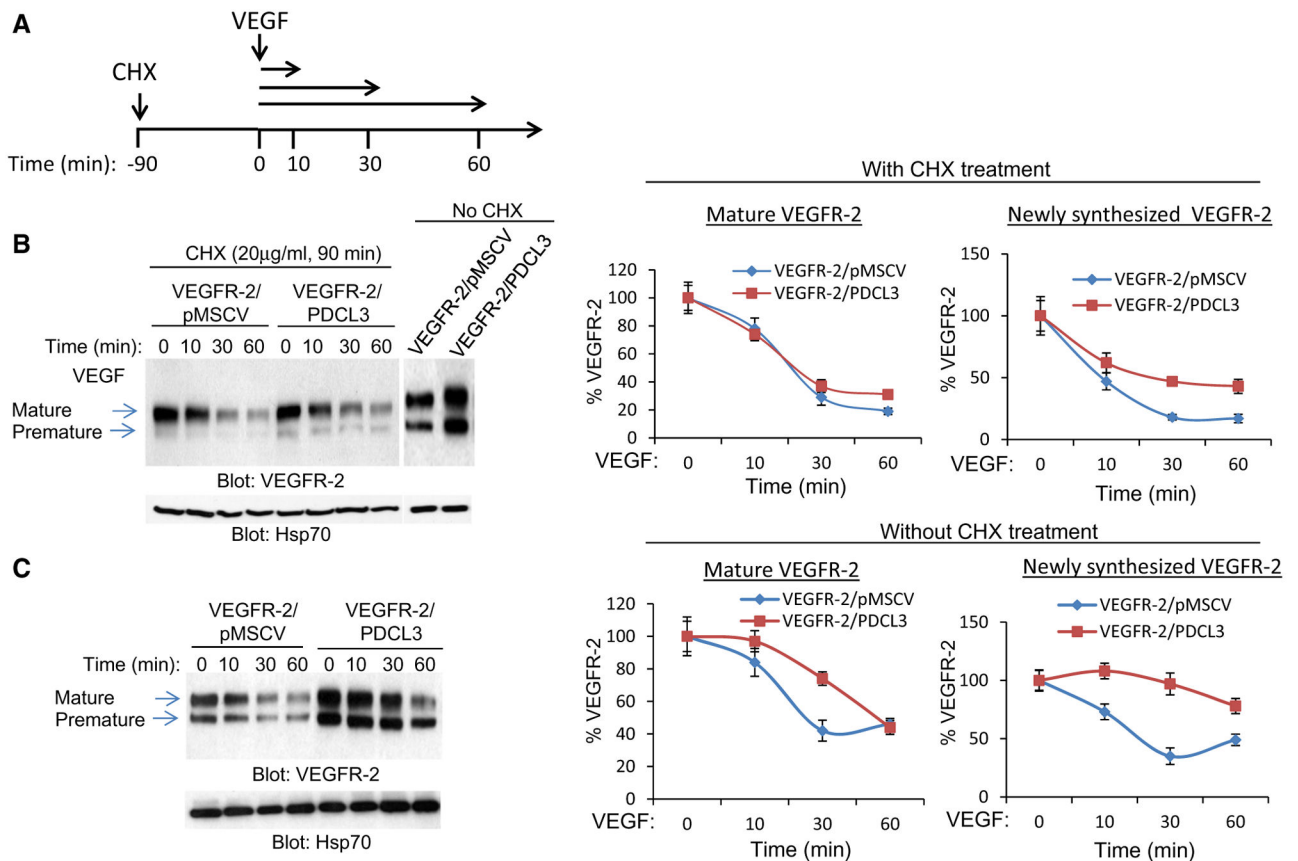
**Fig. 1.**

PDCL3 is localized at the ER and associates with the newly synthesized VEGFR-2: **a** HEK-293 cells expressing VEGFR-2 alone or together with PDCL3 were subjected to cell surface biotinylation as described in “Materials and methods” section. Non-biotinylated and biotinylated fractions were immunoprecipitated (IP) with anti-VEGFR-2 antibody and blotted for PDCL3 using anti-c-Myc antibody. The same membrane was also blotted for VEGFR-2. Non-biotinylated and biotinylated fractions also were blotted for Poly (ADP ribose) polymerase (PARP) a non-cell surface protein as a control. **b** HEK-293 cells were co-transfected with Myc-tagged PDCL3 and VEGFR-2, and after 48 h, they were treated with BFA or control vehicle. Cells were lysed, and whole cell lysates were blotted for VEGFR-2 or were subjected co-immunoprecipitation using anti-c-Myc antibody followed by immunoblotting with anti-VEGFR-2 antibody. **c** HEK-293 cells were co-transfected with Myc-tagged PDCL3 and VEGFR-2, and after 48 h, cells were fixed and subjected to IF staining as described in “Materials and methods” section. **c, d** Cells were stained with anti-PDCL3, anti-c-myc antibodies, or endoplasmic reticulum-specific dye. **d** The overlay of anti-c-Myc with the ER dye also is shown. **e** HEK-293 cells were co-transfected with Myc-tagged PDCL3 and GFP-tagged KDEL, and after 48 h, cells were fixed and subjected to IF staining using anti-PDCL3 antibody or visualized directly for GFP-KDEL. The overlay of PDCL3 with the GFP-KDEL also is shown

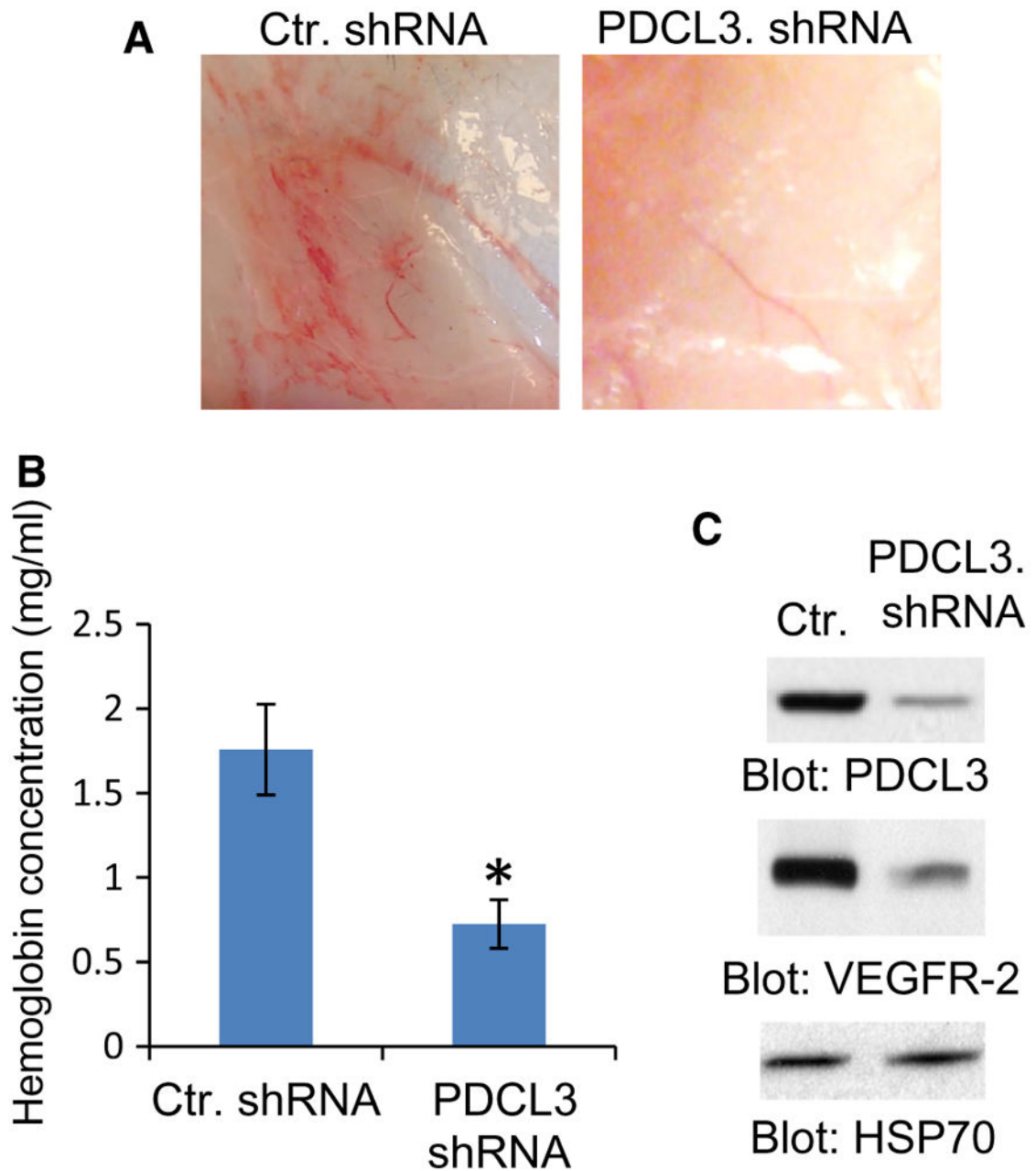


**Fig. 2.** PDCL3 regulates VEGFR-2 expression and folding: **a** HEK-293 cells expressing VEGFR-2 were transfected with different concentrations of C terminus Myc-tagged PDCL3. After 48 h transfection, cells were lysed and whole cell lysates (WCL) were blotted for VEGFR-2, PDCL3 and Hsp70 for loading control. Quantification of premature (newly synthesized VEGFR-2 corresponding to the lower molecular weight) and mature (fully glycosylated and cell surface localized) forms of VEGFR-2 is shown. Mean results of three independent experiments are shown. \* $P = 0.04$  and \*\* $P = 0.15$ . **b** Human umbilical vein endothelial cells (HUVECs) were transfected with control siRNA or PDCL3 siRNA. After 48 h, cells were serum-starved for overnight followed by stimulation with VEGF for 10 min. Cells were lysed, and whole cell lysates were blotted for phospho-Y1054-VEGFR-2, total VEGFR-2, PDCL3 and Hsp70 for loading control. The blots are representative of three independent experiments. **c** In vitro transcription/translation of VEGFR-2 in the absence or presence of exogenous recombinant PDCL3 was performed as described in the “Materials and methods” section, and in vitro-translated VEGFR-2 protein was detected in western blot using anti-VEGFR-2 antibody. The graph representative of two independent experiments is shown. **d** Heat-induced aggregation of VEGFR-2 was measured using PSA fluorescence dye as described in the “Materials and methods” section, and immunoprecipitated VEGFR-2 was used in the presence or absence of PDCL3. The graph represents the mean of two independent experiments with triplicate samples

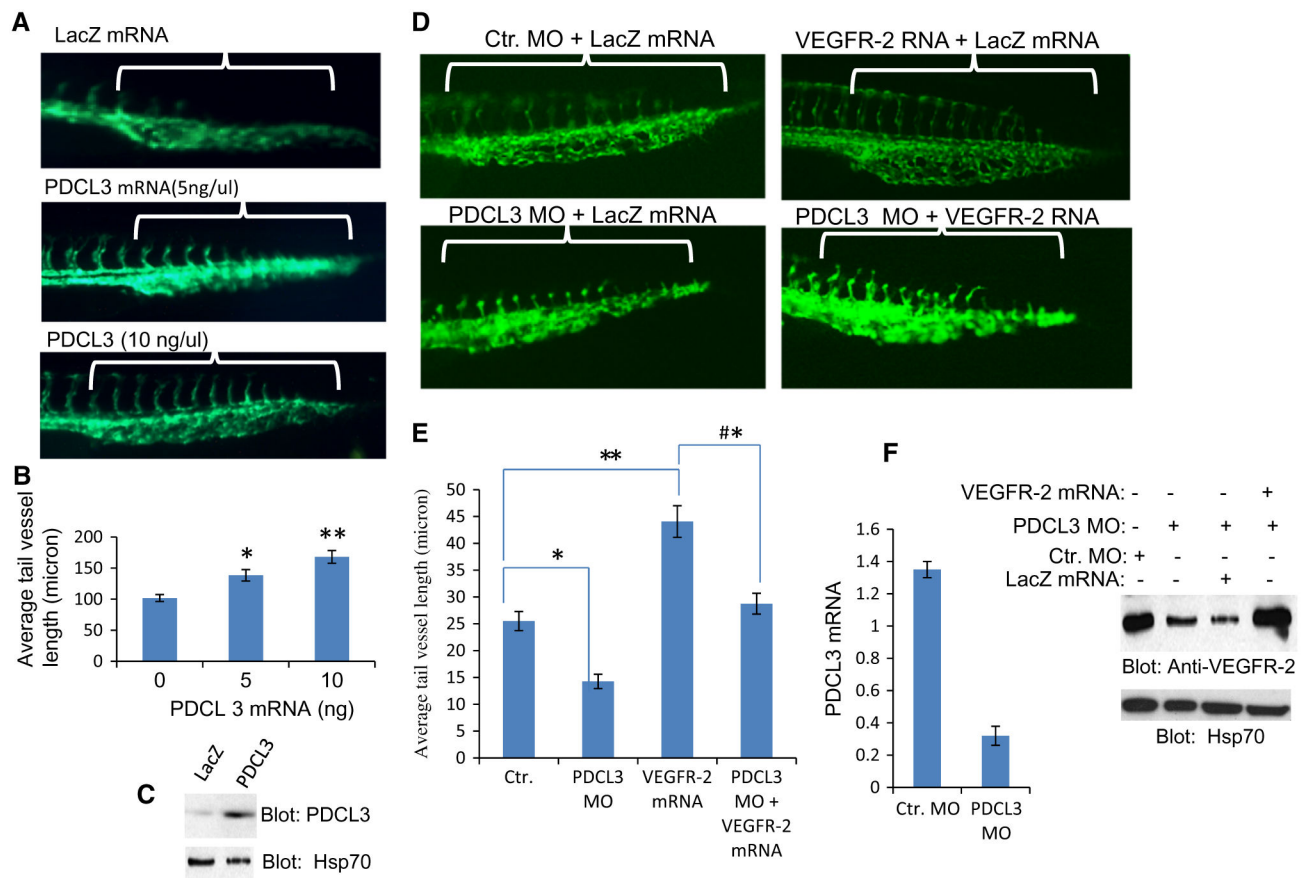


**Fig. 3.**

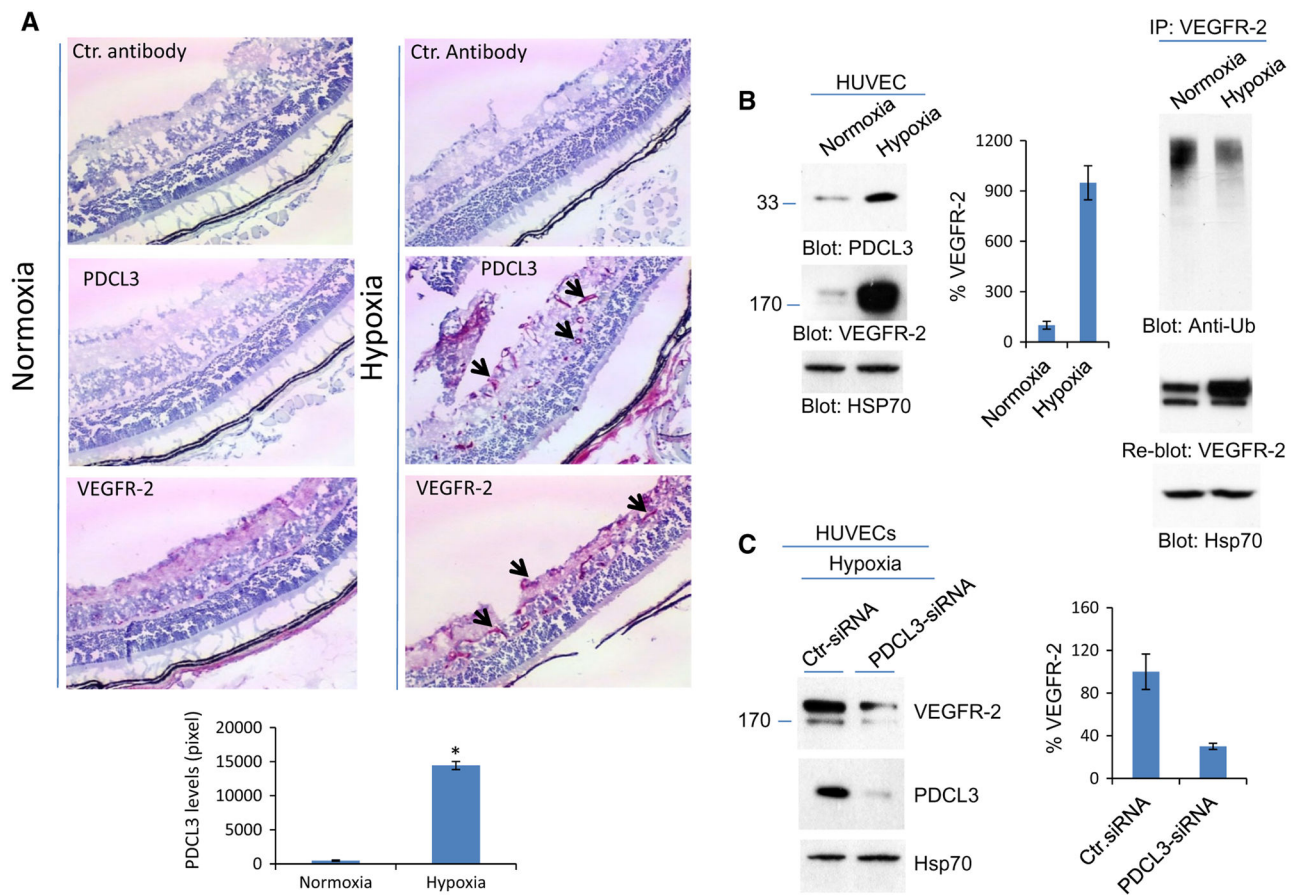
PDCL3 increases the half-life of newly synthesized VEGFR-2: **a** illustrated is the schematic of treatment of cells with cycloheximide (CHX) and VEGF. **b** PAE cells co-expressing VEGFR-2 with empty vector (pMSCV) or PDCL3 were incubated with CHX for 90 min followed by stimulation with VEGF for indicated times. Whole cell lysates were blotted for VEGFR-2 and loading control, Hsp70. Quantifications of half-life of mature VEGFR-2 and premature VEGFR-2 normalized to loading control Hsp70 and are representative of three independent experiments. **c** PAE cells co-expressing VEGFR-2 with empty vector (pMSCV) or PDCL3 were stimulated with VEGF for indicated times without CHX treatment, and whole cell lysates were processed as **a**. Quantification of half-life of VEGFR-2 normalized to loading control is shown. The *graphs* are representative of three independent experiments



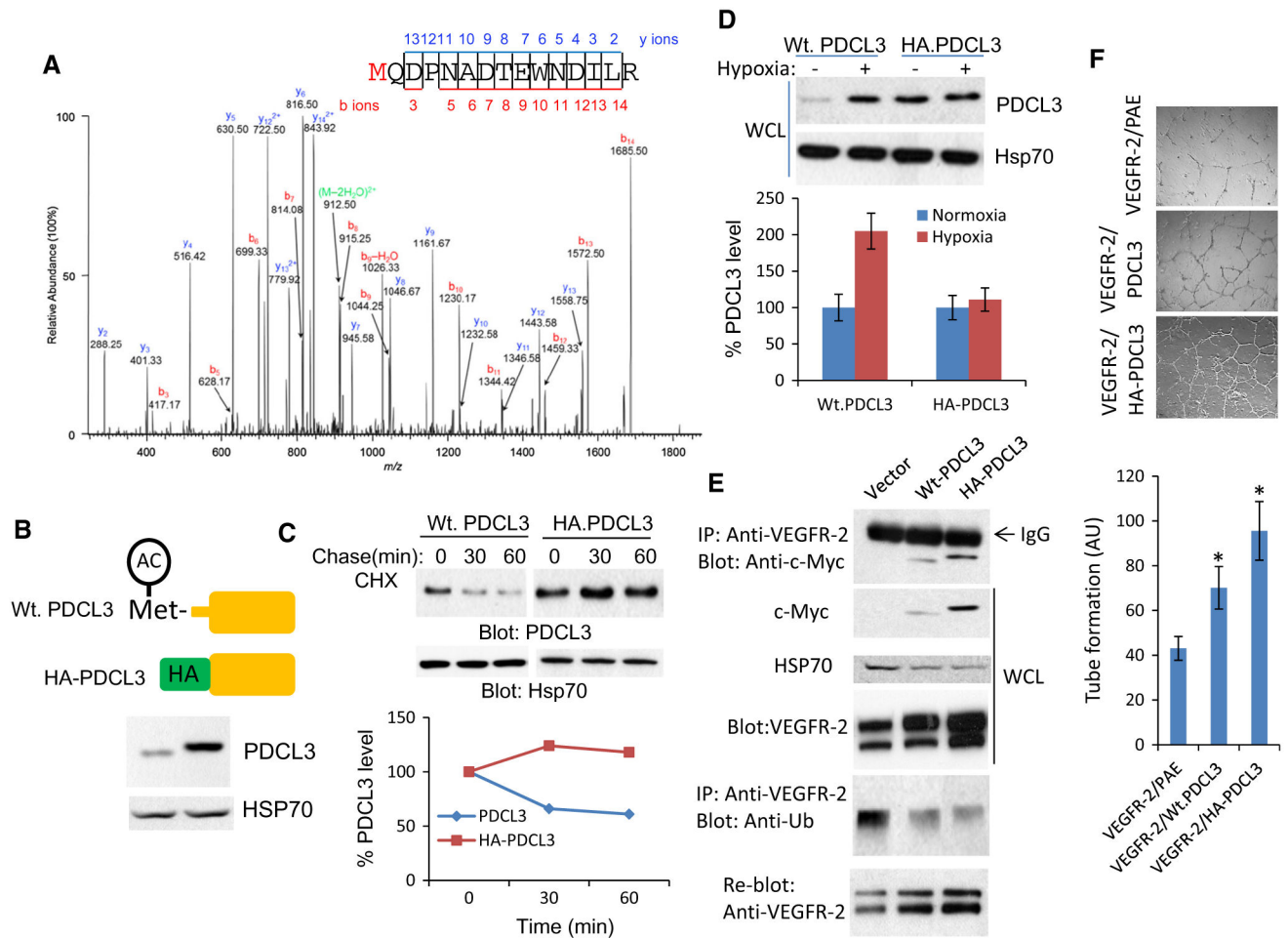
**Fig. 4.** Silencing the expression of PDCL3 inhibits angiogenesis in mouse. **a, b** Matrigel-plug containing VEGF (100 ng), matrigel (10 mg/ml), plus a control retrovirus shRNA or PDCL3 shRNA were injected under skin of mice (6 mice/group). After 8 days, mice were killed, images were taken, and matrigel plugs were removed; hemoglobin content was measured with Drabkin's reagent. The absorbance was read at 540 nm. **c** Matrigel plugs (6 mice/group) were homogenized, and protein extracts were subjected to western blot analysis. Error bars represent SD. \* $P = 0.0401$

**Fig. 5.**

PDCL3 promotes angiogenesis in zebrafish: **a** PDCL3 or LacZ mRNA was injected into one- or two-cell-stage embryos of Fli-eGFP transgenic zebrafish. The embryos were examined after 28 h post-fertilization (hpf), and representative immunofluorescence images are shown. **b** Graph is quantification of intersegmental vessel (ISV) of 10 fishes/group. Error bars represent SD. \* $P = 0.0435$  and \*\* $P = 0.0028$  for 5 and 10 ng PDCL3 mRNA, respectively, compared to control. **c** Western blot analysis of over-expression of PDCL3 from cell lysates of microinjected fishes is shown. Tissue lysates was blotted for PDCL3 and loading control Hsp70. **d** PDCL3 morpholino together with control mRNA (LacZ) or VEGFR-2 mRNA were microinjected into one- or two-cell-stage embryos of Fli-eGFP transgenic zebrafish. Images were taken after 28 hpf, and representative immunofluorescence images are shown. The vessels were marked from the junction of the body and the tail going caudally using Image-Pro<sup>®</sup> and averaged per group, as described in “Materials and methods” section. The tail segment is marked with a *white bracket*. **e** The graph is quantification of ISV formation of 10 fishes/group. Error bars represent SD. \* $P = 0.007$ , \*\* $P = 0.0014$ , and ## $P = 0.001$ . **f** mRNA extracted from fishes (10 fishes/group) of injected with control morpholino (MO) or PDCL3 morpholino and subjected to qPCR and representative graph is shown. Similarly, protein extracts from fishes (10 fishes/group) were lysed and blotted for VEGFR-2 and Hsp70 for loading control

**Fig. 6.**

Hypoxia regulates the expression of PDCL3 in endothelial cells: **a** Mouse hypoxia-induced ocular neovascularization was performed as described in “Materials and methods” section. Immunohistochemistry staining of the postnatal day 17 (P17) of normal mouse eye tissue (normoxia) and hypoxia-induced angiogenesis of mouse eyes was stained for PDCL3 and VEGFR-2. The staining of PDCL3 was quantified using Image J software. The *graph* is the representative of three slides per group. *Error bars* represent SD.  $*P = 0.032$ . **b** Human umbilical vascular endothelial cells (HUVECs) were incubated in hypoxic condition or in normal oxygen (normoxia) for 48 h. Cells were lysed, and whole cell lysates (WCL) was blotted for PDCL3, VEGFR-2, and Hsp70. Also, cell lysates from the same groups were immunoprecipitated with an anti-VEGFR-2 antibody and blotted for ubiquitin using anti-ubiquitin (FK2) antibody. The same membrane was blotted for VEGFR-2. Whole cell lysates from the same groups was blotted for HSP70. *Graphs* are the quantification of the expression of PDCL3 and VEGFR-2 representative of three independent experiments. **c** HUVECs were transfected with either control siRNA (ctr. siRNA) or PDCL3 siRNA, and after 24 h, cells were incubated in hypoxic condition for overnight. Cells were lysed, and whole cell lysates were blotted for VEGFR-2, PDCL3, and Hsp70. *Graph* is representative of three independent experiments

**Fig. 7.**

PDCL3 undergoes N-terminal methionine acetylation: **a** Shown is the mass spectra of acetylated PDCL3 peptide. PAE cells expressing Myc-tagged PDCL3 was immunoprecipitated with anti-Myc antibody and subjected to mass spectrometry analysis as described in “Materials and methods” section. **b** Shown is the schematic of the HA-tagged N terminus methionine mutant PDCL3 and wild-type PDCL3 and their expression in PAE cells. **c** Pulse-chase analysis (CHX, 20  $\mu$ g/ml) of wild-type and HA-tagged methionine mutant PDCL3 is shown. HEK-293 cells expressing wild-type PDCL3 and HA-tagged mutant PDCL3 were incubated with CHX as indicated, cells were lysed, and whole cell lysates (WCL) was blotted for PDCL3 or loading control, Hsp70. Quantification of the same blot also is shown. The blots are representative of two independent experiments. **d** PAE cells expressing wild-type Myc-tagged PDCL3 or HA-tagged N terminus methionine mutant PDCL3 were incubated normal or hypoxic conditions, and after 48 h, cells were lysed and whole cell lysates were blotted for PDCL3 and loading control, Hsp70. Graph is representative of two independent experiments. **e** Cell lysates from HEK-293 cells co-expressing myc-tagged PDCL3 with VEGFR-2 or HA-PDCL3 with VEGFR-2 were immunoprecipitated with anti-VEGFR-2 antibody and immunoblotted for PDCL3 using anti-Myc antibody. Whole cell lysates were also blotted for VEGFR-2, PDCL3, and Hsp70

as a loading control. Ubiquitination of VEGFR-2 was determined by immunoprecipitation with anti-VEGFR-2 antibody followed by immunoblotting with anti-ubiquitin antibody. The *blots* are representative of two independent experiments. **f** PAE cells expressing VEGFR-2 alone and co-expressing with wild-type PDCL3 or HA-tagged PDCL3 were subjected to tube formation assay, and images were taken after overnight. Tube formations were quantified by NIH Image J program using three randomly selected areas per group. *Error bars* represent SD. \* $P = 0.005$